Importance of carrier dynamics and conservation of momentum in atom-selective STM imaging and band gap determination of GaAs(110)

N. D. Jäger,[1] E. R. Weber,[2] K. Urban,[1] and Ph. Ebert[1]
[1]*Institut für Festkörperforschung, Forschungszentrum Jülich GmbH, 52425 Jülich, Germany*
[2]*Dept. of Materials Science, University of California, and Materials Sciences Division, Lawrence Berkeley National Laboratory, Berkeley, California 94720*
(Received 18 November 2002; published 29 April 2003)

Scanning tunneling microscopy and spectroscopy measurements on the GaAs(110) surface with complementary theoretical calculations are performed to clarify the effects involved in the tunneling of unpinned semiconductor surfaces. We show that the flatband and tip-induced band bending as well as equilibrium conditions are insufficient to describe the effects involved. Instead, carrier dynamics and conservation of momentum of the tunneling electrons need to be taken into account for a complete description of the contributions of the valence or conduction band states. The results allow us to understand the unique properties needed to achieve the atom-selective imaging observed on these surfaces as well as the determination of the band gap energy.

DOI: 10.1103/PhysRevB.67.165327 PACS number(s): 73.40.Ei, 68.37.Ef

I. INTRODUCTION

Chemically sensitive scanning tunneling microscopy has attracted wide interest, but only a limited number of successful examples demonstrated the ability to distinguish different types of atoms within a surface.[1–9] One of the most prominent example is the (110) cleavage surface of III-V semiconductors, where anions and cations can be imaged separately.[10] This so-called atom-selective imaging is possible because at negative sample voltages electrons tunnel from occupied dangling bonds localized above the anions into empty tip states, whereas at positive voltages electrons tunnel from filled tip states into the unoccupied dangling bonds above the cations.[10,11] However, this simple picture assumes flat bands, neglecting the presence of a band bending due to the proximity of the tip and applied voltage. For negative sample voltages, the tip-induced band bending leads eventually to a population by electrons of the initially empty cation-derived dangling bonds states in the conduction band. Since these occupied conduction-band states encounter a lower-vacuum barrier than the occupied valence-band states, scanning tunneling microscopy images of the occupied surface states should predominantly show the cation-derived dangling bonds in the conduction band and not the anion-derived dangling bonds in the valence band. Thus atom-selective imaging should be impossible on (110) surfaces of III-V semiconductors in obvious contrast to experimental observations.[10,12,13]

In order to solve this inconsistency, we resumed the scanning tunneling microscopy (STM) and spectroscopy (STS) measurements on GaAs(110) with complementary calculations to clarify the effects involved. We show that carrier dynamics and the conservation of momentum of the tunneling electrons are crucial to allow an atom-selective imaging of these surfaces. We identify the properties of materials which would lead to the imaging of conduction-band states at all applied voltages. Furthermore, we demonstrate how to determine accurately the magnitude of the band gap energy from scanning tunneling microscopy data.

In this paper we first present the details of our experiments (Sec. II) and our calculations (Sec. III). In Sec. IV we present STM and STS results on *n*-type GaAs, followed by a detailed discussion (Sec. V). This discussion is divided into (A) tunneling into empty states, where the results of (residual *n*-type) semi-insulating and highly *n*-doped material differ significantly, and (B) tunneling out of filled states. In Sec. VI we present our results on *p*-type GaAs along with a detailed discussion. Our findings on *n*-type and *p*-type conducting materials allow us in Sec. VII to present a method on how to determine the band gap energy.

II. EXPERIMENT

For the present work we investigated various highly *n*-doped GaAs samples with silicon dopant concentrations ranging from 1×10^{18} to 4×10^{18} cm^{-3} and *p*-doped GaAs samples with zinc acceptor concentrations from 3×10^{16} to 3×10^{19} cm^{-3}, as well as semi-insulating (SI) GaAs containing 1.3×10^{16} cm^{-3} EL2 deep donors[14] for comparison. The samples were cleaved in ultrahigh vacuum to expose a clean and defect-free (110) surface. On these surfaces we acquired scanning tunneling microscopy and spectroscopy data using a homebuilt system[15] similar to that developed by Frohn *et al.*[16] In this design the scanning unit with a high resonance frequency[17] is supported by a Viton stage, which itself is placed into a vacuum chamber supported by pneumatic laminar flow damping isolators. This ensures low-noise current-voltage spectra that were measured either at constant tip-sample separation or at varying tip-sample separation to increase the sensitivity following the method proposed by Feenstra.[18] With the voltage applied to the sample, the STM images on *n*-type GaAs were acquired in the constant-current mode and the images on *p*-type in constant-height mode. Special care was taken to allow the comparison of the registry of images acquired at different voltages.

III. DETAILS OF THE CALCULATION

For a discussion of our results we calculated the positions of the conduction-band (E_{CS}) and valence-band (E_{VS}) edges

at the GaAs surface underneath the tip as well as the resulting tunneling current. We based our calculation of the band edge energies on the one-dimensional integration of Poisson's equation described by Feenstra and Stroscio[19] and Seiwatz and Green,[20] but extended it in two significant aspects. First, the Fermi energy in the bulk was calculated using Fermi-Dirac statistics. Second, the procedure of Refs. 19 and 20 assumes equilibrium conditions for the carrier distribution in the semiconductor. The discussion will show that this assumption is not valid, and therefore we included the effects of carrier dynamics by zeroing the minority and/or majority carrier concentration at the surface. The tunneling current is computed exactly as described by Feenstra and Stroscio[19] and Bono and Good.[21] This model is based on the approach by Tersoff and Hamann[11] and Selloni *et al.*[22] to integrate over all states between the tip and sample Fermi level times the transmission coefficient. Parabolic bands are assumed for the density of valence- and conduction-band states. The transmission coefficient through the vacuum barrier as well as through the semiconductor's space charge region is estimated using the WKB approximation. Thereby the vacuum barrier is taken as trapezoidal modified by the image charge lowering.

Our calculations were performed for 1×10^{18} cm^{-3} Si-doped GaAs and semi-insulating GaAs containing 1.3×10^{16} cm^{-3} deep donors. In both cases a background carbon acceptor concentration of 4.8×10^{14} cm^{-3}, a work function of 4.5 eV for the metallic tip, a tip-sample separation of 0.9 nm, and a tunneling area of 1 nm^2 were assumed.[19] Variation of these parameters does not change the results qualitatively.

IV. EXPERIMENTAL RESULTS FOR *n*-TYPE CONDUCTING GaAs

In Fig. 1 we show two different current-voltage (I-V) curves obtained on the (110) surfaces of highly *n*-doped GaAs. For comparison we also show one data set acquired on semi-insulating GaAs that has residual *n*-type conduction.[14] The curves exhibit a number of characteristics: (i) All current-voltage curves essentially overlap for sample voltages $V<-2$ V. (ii) At positive voltages the I-V curves of the highly *n*-doped materials essentially overlap. In contrast, on semi-insulating GaAs no current can be obtained below $+5$ V. (iii) The current obtained between 0 and -1.5 V differs considerably between different I-V measurements on the highly *n*-doped GaAs(110) surfaces. The two I-V curves shown are chosen as examples to highlight the effect of the tip dependence. This is not an effect of the variation of the doping level of the samples.

Figure 2 shows a set of correlated high-resolution STM images of the highly *n*-doped GaAs(110) surface acquired at different voltages. The box marks a unit cell whose position relative to the atomic lattice is the same in each image. Two effects are visible: (i) the morphology and orientation of the apparent atomic rows is rotating and (ii) the maxima are spatially shifting as a function of the voltage.

(i) For positive voltages the corrugation is strong along the $[1\bar{1}0]$ direction and thus the atomic rows appear oriented along the [001] direction. For small magnitudes of negative voltage [Fig. 2(b)] the corrugation is essentially the same as for positive voltage and the obtained image is barely distinguishable from Fig. 2(a). At high magnitudes of negative voltage the STM image displays a strong corrugation along the [001] direction and hence the atomic rows appear to be oriented along the $[1\bar{1}0]$ direction.

(ii) Note the shift of the maxima of half a unit cell along the $[1\bar{1}0]$ direction and of approximately 1/3 of a unit cell along the [001] direction between the image taken at positive sample voltage and the image taken at -3.5 V.

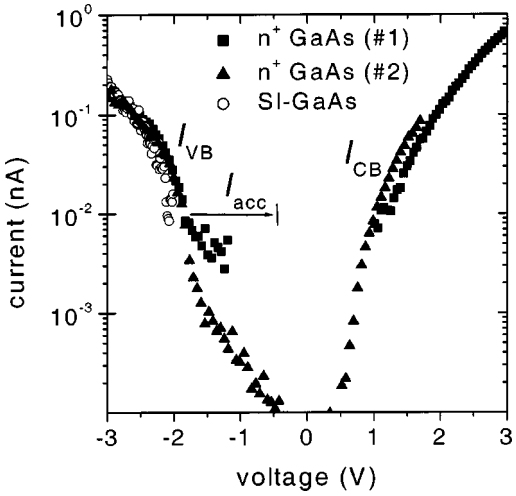

FIG. 1. Current-voltage data obtained in two measurements of highly *n*-doped GaAs (■, ▲) and one curve obtained on semi-insulating GaAs (open circles). At positive voltages current is only observed on highly *n*-doped GaAs, not on semi-insulating GaAs. This current, I_{CB}, is due to electrons tunneling into the conduction band. At negative voltages the currents originate from the accumulation layer, I_{acc}, and from the valence band, I_{VB}.

V. DISCUSSION FOR *n*-TYPE CONDUCTING GaAs

For the discussion we recall that at positive (negative) voltages, a flow of tunnel current requires that the tip's occupied (empty) states must energetically face the empty (filled) states of the sample. This requirement is nontrivial for semiconductors because of the band gap and the presence of a tip-induced band bending. At first we briefly discuss the situation with no tip-induced band bending.

Current-voltage spectroscopy without any tip-induced band bending would exhibit at negative voltages current arising from the sample's filled valence-band states and at positive voltages current due to electrons tunneling into the empty conduction-band states. The region in between with no current should then have a width in voltage reflecting the band gap energy. However, this is mostly not observed as one can see also in Fig. 1 and in previous measurements.[19,23] First, the obvious differences between semi-insulating and highly *n*-doped GaAs show that one cannot extract the size of the band gap E_g from the tunneling spectra as straightforward as implied previously. Second, clearly a current can be detected between -1.4 V$<V<0$ V, which makes it difficult

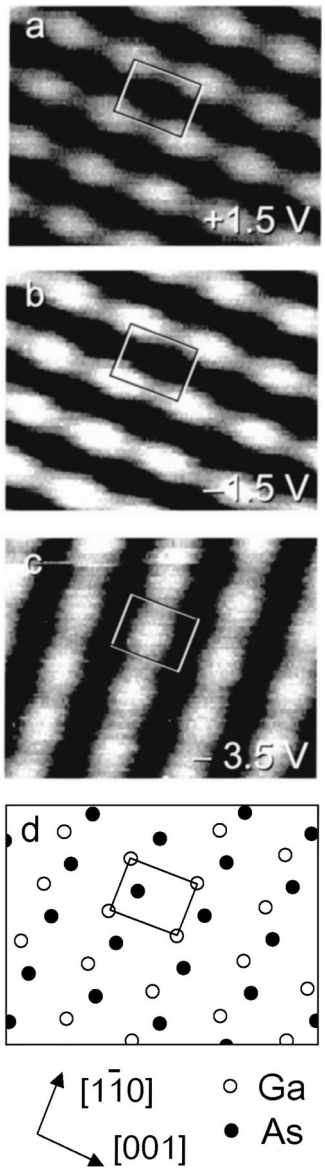

FIG. 2. (a)–(c) STM images of the (110) surface of highly *n*-doped GaAs taken at various sample voltages indicated in the images. (d) Schematic drawing of the arrangement of the Ga (○) and As (●) atoms in the top layer of the GaAs (110) surface. The location of the box marks equal relative positions to the lattice in each image. It spans the size of a GaAs unit cell of 0.56 nm by 0.4 nm.

to define properly the onset of the band edges, which should be $E_g/e = 1.42$ V apart, with e being the elemental charge. Thus an interpretation with no tip-induced band bending is not correct. The necessity to include tip-induced band bending for the description of tunneling on semiconducting materials has been addressed previously.[19,23] However, we will show in the following that equilibrium conditions assumed for the calculation of the amount of band bending are insufficient to describe tunneling at positive sample voltages (empty states images) for semi-insulating GaAs and highly *n*-type GaAs. Afterwards, we address tunneling at negative sample voltages (filled state images) and in the band gap region, where we will show that plain Tersoff-Hamann

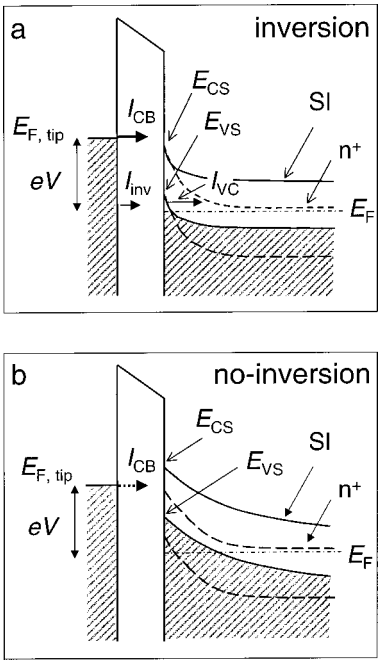

FIG. 3. Schematic band diagram of the metal-tip–vacuum–semi-insulating (SI) and highly doped (n^+-)GaAs tunneling junction at positive sample voltages (eV). (a) Equilibrium case with free holes gathered in the valence band at the surface (inversion). An electron current flows from the tip states to the conduction-band states of the semiconductor (I_{CB}) and to the inversion layer (I_{inv}). I_{VC} denotes the current from the inversion layer to the conduction band. (b) Case without inversion. An electron current from the tip to the sample flows only for n^+-GaAs. Note the schematic is not to scale. The extend of the band bending is much larger than the vacuum barrier width. E_{CS}, E_{VS}, $E_{F,tip}$, and E_F, are the conduction-band edge at the surface, valence-band edge at the surface, tip's Fermi level, and sample Fermi level, respectively.

theory[11] cannot describe the details of the states involved in the tunneling current.

A. Tunneling into empty states of *n*-type conducting GaAs

The current-voltage spectrum of Fig. 1 shows that the spectra of *n*-doped and semi-insulating GaAs are significantly different for positive sample voltages, whereas they are matching for negative sample voltages of $V < -2$ V. The same tendency has been observed for doping concentrations ranging from 10^{16} to 10^{18} cm^{-3}.[23]

1. Semi-insulating GaAs with residual n-type conduction

At positive voltages, tunneling current flows if the tip's Fermi level ($E_{F,tip}$) is energetically above the conduction-band edge of the surface underneath the tip (E_{CS}). The observation of no tunneling current in the case of semi-insulating GaAs thus implies that the conduction-band edge (E_{CS}) is always above the tip's Fermi level ($E_{F,tip}$) as schematically outlined in Fig. 3(b). In equilibrium this condition would not prevail, because if the valence-band edge at the surface (E_{VS}) is above the sample's Fermi level (E_F), holes will gather at the surface and an inversion will develop. This

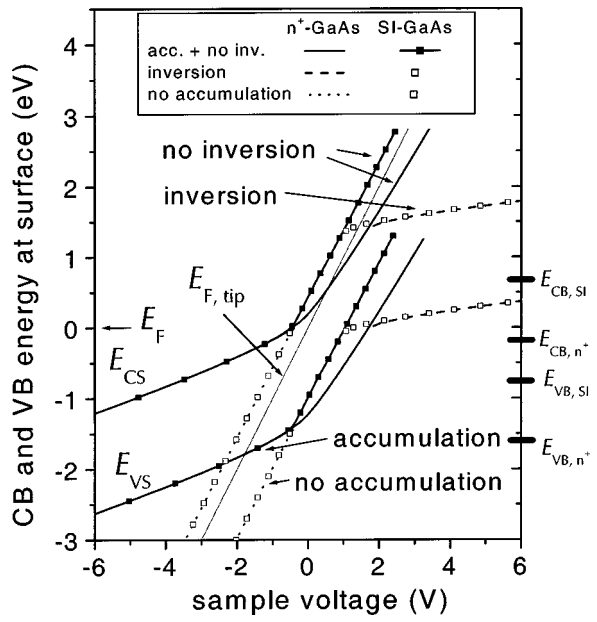

FIG. 4. Calculation of the conduction-band (E_{CS}) and valence-band (E_{VS}) edge energies at the semiconductor surface of a metal-vacuum-GaAs system as a function of applied sample voltage. Several cases are shown for highly *n*-doped (n^+) and semi-insulating (SI) GaAs: with and without accumulation at negative sample voltages and with and without inversion at positive voltages. Indicated by the bars on the right axis are the energetic positions of the bulk valence-E_{VB}, and conduction-band E_{CB}, edges, for the two materials. The Fermi level of the tip ($E_{F,tip}$) lies on the dotted diagonal. All energies are given relative to the Fermi level of the sample.

limits the band bending to about +0.7 eV and allows filled tip states to face empty conduction-band states [Fig. 3(a)]. The resulting band edge locations can be illustrated better with results of our calculation of the surface conduction- and valence-band edges as a function of sample voltage (Fig. 4). Although these calculations are based on a one-dimensional model, the main features can be discussed correctly. For semi-insulating GaAs and small positive bias ($0<V<+0.7$ V) the electric field of the tip is screened by charged deep donors. The conduction-band edge (E_{CB}) rises almost directly with the applied bias and therefore always stays above the tip's Fermi level ($E_{F,tip}$) (Fig. 4, ■). For voltages greater than about +0.7 V, the valence-band edge (E_{VS}) crosses the sample's Fermi level. At this point under equilibrium conditions, inversion sets in and the band edge positions essentially remain fixed (open squares). Thereby the tip's Fermi level ($E_{F,tip}$) rises above the conduction-band edge, in which case tunneling would be allowed. Without inversion (■) the bands continue to rise directly with the applied voltage and thus the conduction-band edge always stays above the tip's Fermi level. Hence one can conclude that inversion does not occur in semi-insulating GaAs.

2. Highly n-doped GaAs

In contrast to semi-insulating GaAs a tunneling current is detected at positive voltages on highly *n*-doped GaAs [Figs. 1 and 2(a)]. The STM images at low positive voltages exhibit apparent rows predominantly oriented along the [001] direction [Fig. 2(a)]. This is the signature of the dangling bond or C_3 state in the conduction band, which is the lowest-lying conduction-band state imaged.[24,25] The occurrence of a tunneling current on highly doped *n*-GaAs indicates that the screening of the tip's electrical field must be more effective than in the case of semi-insulating GaAs, such that the tip-induced band bending is smaller. This could be either due to the possible existence of an inversion near the surface or due to the higher density of dopant atoms. The band edge energies for highly doped *n*-type GaAs are calculated in Fig. 4 for both cases: screening only by dopants (no inversion, solid lines) and screening with the presence of inversion (dashed lines). For voltages below about +1.8 V both curves are identical, as the field is only screened by charged dopants. For higher voltages, inversion causes the bands to remain at 1.5–2 eV above their bulk values ($E^+_{CB,n}$,$E^+_{VB,n}$), whereas the bands continue to rise in case of screening solely by donors (solid line). In contrast to the semi-insulating case, the tip's Fermi level ($E_{F,tip}$) is above the conduction-band edge (E_{CS}) already for voltages as small as +0.5 V well before inversion sets in. This permits tunneling of electrons from the tip into the empty conduction-band states for either case—i.e., with as well as without inversion [Fig. 3(a), dashed lines]. The reason is the high density of dopants that can screen the field of the tip effectively. In the following we will show on the basis of experimental as well as theoretical arguments that inversion does neither take place for highly doped material.

3. Absence of inversion

Due to the high density of valence-band states, the screening of the tip's electric field is, in case of inversion, largely dominated by screening by holes in the valence band at the surface, because the hole concentration is much larger than the dopant concentration. As a consequence, the tip-induced band bending levels at 1.5–2 eV (Fig. 4, above +1.5 V), because small band bending changes induce large changes in the hole concentration. The saturation of the band bending leads to a sudden increase of the number of conduction-band states facing filled tip states. Thus the tunnel current would be expected to increase suddenly once inversion takes place. This would lead to a kink in the current at the onset of inversion (about +1.5 eV) as can be seen in the calculation of the tunneling current in Fig. 5. However, such a kink cannot be observed experimentally (Fig. 1), in agreement with previous data.[19] The absence of inversion can be further corroborated on the basis of the doping-dependent measurements. As shown in Fig. 4, the positions of the valence- and conduction-band edges at the surface are in the case of inversion independent of the donor concentration. Thus the tunnel current at larger positive voltages should be independent of the doping concentration. This disagrees with our results (Fig. 1) and with previous studies.[23] In summary, there is no experimental indication of inversion taking place.

This conclusion can be further corroborated theoretically. If inversion is present, electrons should be able to tunnel into the emptied valence-band states at the surface. We calculated

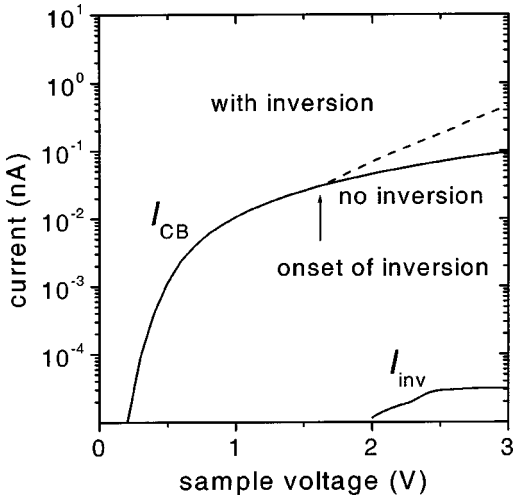

FIG. 5. Calculated tunneling currents for the metal-tip–vacuum–n^+-doped GaAs tunneling junction at positive sample voltage. I_{CB} denotes the electron current from the tip in to empty conduction-band states of the semiconductor. Two cases are shown for higher voltages: tunneling with the possibility of inversion (dashed line) and without inversion (solid line). The tunneling current of electrons tunneling from the tip to the empty valence band states in case of inversion [see Fig. 3(a)] is denoted I_{inv}.

that this current (I_{VB}) is about 3.5 orders of magnitude smaller than the current into the conduction band (I_{CB}) as shown in Fig. 5 due to the larger vacuum barrier. Nevertheless, this current must be maintained by holes reaching the inversion zone at the surface. Otherwise, the inversion breaks down. There are two channels by which holes could reach the surface: transport by drift from the bulk valence band or electrons tunneling from the valence band to the conduction band through the semiconductor's space charge region [see I_{VC} in Fig. 3(a)].

We first discuss the first channel. The maximum drift current density that can be expected by transport is $J_h = e\,\nu_{h,\max} p$, with e being the elemental charge, $\nu_{h,\max}$ the maximum drift velocity of holes, and p the hole concentration in the bulk. The hole concentration is given by $p = n_i^2/n$, with n_i the intrinsic carrier concentration and n the concentration of free electrons. If we assume drift velocities in the order of $\nu_{h,\max} = 1\times10^7$ cm/s (Ref. 26) and free electron concentrations of $n = N_D$, the donor concentration, we obtain a current density of not more than 10^{-8} nA cm^{-2}. This is 19 orders of magnitude smaller than the current density of the tunnel current into the emptied valence-band states (more than 10^{11} nA cm^{-2}). Thus even a geometric factor (localized tip) or a lower free electron concentration cannot increase the drift current enough to accommodate the transport of the holes necessary to maintain inversion.

The second channel, which would allow holes to reach the surface, is based on electrons tunneling from the valence-band states through the space charge region into conduction-band states [I_{VC} in Fig. 3(a)]. Using the WKB approximation, we calculated the transmission coefficient for this path to be about 5×10^{-26} for electrons at the top of the surface valence-band edge and at $+3$ V sample voltage. This value is significantly smaller than the transmission coefficient for electrons tunneling from the tip into the emptied valence-band states at the surface of about 5×10^{-8}, because the width of the depletion zone of about 40 nm is much larger than that of the vacuum barrier of 0.9 nm. Therefore, an inversion cannot be maintained by electrons tunneling from the inversion layer through the space charge region into the bulk conduction-band states.

The above discussion shows that no inversion occurs on *n*-type GaAs or semi-insulating GaAs in the STM configuration at positive voltages. This is only due to the fact that under tunneling conditions, no equilibrium state is reached. The tunnel current is largely determined by the carrier dynamics in the GaAs samples. Because the tip's field is only screened by charged donors, the conduction-band edge position at the surface as well as the magnitude and onset of the tunneling current is dependent on the doping concentration at positive sample voltage, as observed experimentally.

B. Tunneling out of filled states of *n*-type conducting GaAs

1. Presence of an accumulation layer

At large magnitudes of negative sample voltages the measured currents essentially do not differ for a broad range of doping concentrations from semi-insulating to highly doped GaAs (Fig. 1). This is corroborated by Ref. 23. Therefore the energetic position of the valence-band edge shifted by the tip-induced band bending has to be alike for all doping concentrations. Thus the screening mechanism must be similar, independent of the doping level. In principle, there are two screening mechanisms for negative sample voltages: screening by residual acceptors or by free electrons accumulated at the surface.

The concentration of residual acceptors in *n*-doped GaAs is typically below 10^{15} cm^{-3}. Thus, if the tip's field is solely screened by charged acceptors with such low concentrations, one would expect a strong band bending. We also calculated that in this case the tip's Fermi level ($E_{F,\mathrm{tip}}$) would energetically always be above the valence-band edge at the surface (dotted line in Fig. 4), yielding a situation as shown schematically in Fig. 6(b). Thus no filled valence-band states face empty tip states and no current can be extracted from the valence-band states. Since we assumed only screening by charged acceptors and not by free electrons accumulated at the surface, the conduction-band states remained empty and no current can be extracted from those states either, although the tip's Fermi level $E_{F,\mathrm{tip}}$ would be below the conduction-band edge E_{CS} [Fig. 6(b)]. However, the clear observation of a tunnel current at negative voltages (Figs. 1 and 2) requires filled semiconductor states to face empty tip states. This can only occur if free electrons accumulate at the surface for all doping concentrations including semi-insulating GaAs.

Further evidence for electron accumulation at the surface is found in the current-voltage data of Fig. 1 and Ref. 19 as well as in the STM images of Fig. 2. Figure 1 shows that a current can be detected for voltages in the range of $-0.5\ \mathrm{V} > V > -1.4\ \mathrm{V}$, i.e., at voltages for which the tip's Fermi level is above the bulk valence-band edge and in the GaAs band gap. Since no surface states exist in the band gap, all

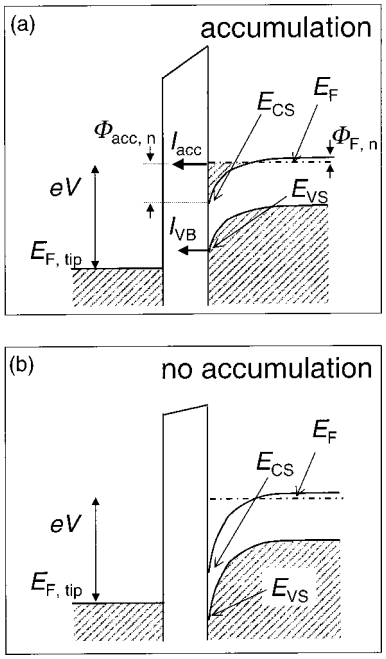

FIG. 6. Schematic band diagram of the metal-tip–vacuum–*n*-doped GaAs tunneling junction at negative sample voltages (eV): (a) equilibrium case with free electrons gathered in the conduction band at the surface (accumulation) and (b) case without accumulation. Note the schematic is not to scale: The extent of the band bending is much larger than the vacuum barrier width. I_{acc} and I_{VB} denote the current from the conduction band and from the valence band to the empty tip states, respectively. E_{CS}, E_{VS}, $E_{F,tip}$, and E_F, are the conduction-band edge at the surface, valence-band edge at the surface, tip's Fermi level, and sample Fermi level, respectively. $\Phi_{acc,n}$ is the difference in the band edge energies at the surface and the bulk. $\Phi_{F,n}$ is the difference between the Fermi level and the conduction-band edge in the bulk.

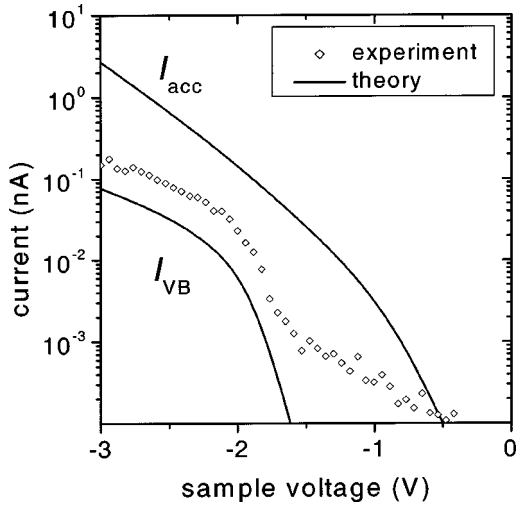

FIG. 7. Calculated tunneling currents for the metal-tip–vacuum–n^+-doped GaAs tunneling junction at negative sample voltages compared to the experimentally observed current ($\diamond$). I_{acc} denotes the electron current originating from the accumulation layer [see Fig. 6(a)]. I_{VB} denotes current originating from the valence band.

current in this voltage range must originate from conduction-band states. This is corroborated by the contrast and registry of the STM image measured at -1.5 V [Fig. 2(b)]. In both images the apparent rows of maxima are oriented along the [001] direction and the maxima appear at nearly exactly the same spatial positions (see box in Fig. 2). We conclude from this that Figs. 2(a) and 2(b) show both the C_3 state. In Fig. 2(a) electrons tunnel into the empty C_3 state, whereas in Fig. 2(b) electrons tunnel out of the C_3 state occupied by free electrons due to the presence of the accumulation layer. Thus an accumulation layer exists under tunneling conditions.

In equilibrium conditions an accumulation layer develops for voltages at which the conduction-band edge at the surface E_{CS} is equal to or below the sample's Fermi level E_F. This happens at voltages of $V \approx -(\Phi_m - \chi_{SC})/e \approx -0.5$ V, with Φ_m being the metal work function, χ_{SC} the semiconductor's electron affinity, and e the elemental charge. Thus tunneling of electrons from the accumulation layer can be expected to start for voltages $V < -0.5$ V (I_{acc} in Fig. 7).

2. Valence-band contributions to the tunnel current

In the presence of an accumulation layer at the surface in the STM configuration, the band bending is determined by the density of states of the conduction-band states and not anymore by the dopant atom concentration, because the latter is much smaller than the density of states of the conduction band. As a result, the band bending and energetic positions of the band edges at the surface are only weakly dependent on the applied voltage (Fig. 4). Thus the valence-band edge at the surface, E_{VS}, is above the Fermi level of the tip $E_{F,tip}$ for voltages $V < -1.75$ V (Fig. 4), where our calculations show a tunneling current out of the valence band [I_{VB} in Figs. 6(a) and 7]. Therefore, the tunnel currents seen at negative voltages $V < -1.75$ V are practically identical for all doping concentrations, in agreement with the experimental current-voltage data of Fig. 1 and Ref. 23.

Experimentally, the current out of the valence band is evident in the STM images as well as in the current-voltage data. The experimental current-voltage curves on highly *n*-doped GaAs (see Fig. 1 and Ref. 19) show a shoulder at the expected voltage (≈ -1.75 V) for the onset of the valence-band current. We also find at higher negative sample voltages that the imaged maxima [Fig. 2(c)] display a shift of about $a/3$ in the [001] and $a/(2^{3/2})$ in the $[1\bar{1}0]$ direction compared to the images at low negative voltages as well as positive voltages [Figs. 2(a) and 2(b)], with a being the lattice constant. Obviously, the surface states imaged at low and high negative voltages are not the same. The shift in registry corresponds exactly to the shift expected between the anion and cation sublattices. In addition, the strong corrugation along the [001] direction leading to apparent atomic rows in $[1\bar{1}0]$ direction in Fig. 2(c) indicates that the anion-derived occupied A_5 dangling bond state in the valence band is imaged at *high magnitudes* of negative voltages,[24,25] whereas the C_3 state is imaged at *small magnitudes* of negative voltages. From these results it becomes obvious that the so-called atom-selective imaging[10]—i.e., the observation of the change in registry between states in the conduction- and

valence-band states—is only possible for carefully selected voltages. This is because at low negative voltages the current is carried by electrons tunneling out of filled conduction-band states, whereas at high negative voltages the tunnel current is dominated by electrons tunneling out of valence-band states.

3. Importance of carrier momentum

It is important to realize that the experimentally observed tunneling current at sufficiently high negative voltages is composed of electrons tunneling out of the accumulation layer *and* tunneling out of valence-band states. However, the experimentally observed domination of the valence-band current is in contrast to theoretical expectations: The current out of the conduction-band states, I_{acc}, should be at least one order of magnitude larger than the current out of the valence band, I_{VB} (see Fig. 7). This is due to the fact that electrons tunneling out of the conduction-band states feel a smaller vacuum barrier height as compared to those tunneling out of the valence-band states [see Fig. 6(a)]. Therefore, one would expect I_{CB} to dominate at any negative sample voltage. This is in contrast to the experimental observation that tunneling out of valence-band states dominates at sufficiently large negative voltages.

There are several possible reasons for the tunneling current component out of the conduction band to be significantly smaller than expected: a kinetic limitation in the transport of free electrons to the surface, a limitation by the thermalization of these electrons into the accumulation layer, or a reduced tunneling probability through the vacuum barrier. We do not expect the first two reasons to be tip dependent. In addition, the transport of free electrons toward the surface can be estimated in analogy to the drift of holes at positive voltages. A rough estimate shows that the drift current is high enough for all doping levels investigated, because the free electrons are majority carriers. Thus the drift is not the rate limiting factor. This leaves the possibility of a reduced tunneling probability.

In the tunneling transmission coefficient of our model used, which is essentially based on the Tersoff-Hamann approach of interpreting STM images,[11] we only considered the energy dependence, but neglected momentum conservation. The momentum of electrons tunneling from the surface through the vacuum barrier to the tip must be conserved: i.e., the tip must have states able to accommodate electrons with a given momentum. The lowest-lying C_3 surface state on the (110) surface of most III-V compound semiconductors is located at the $\bar{X}$ point of the surface Brillouin zone.[27–32] The wave vector **k** of this state has a nonzero momentum parallel to the semiconductor surface, unlike electrons from the top of the valence band, which are at the $\bar{\Gamma}$ point. We propose that therefore tunneling out of the accumulation layer is hindered by the inability of sharp tips to accommodate this momentum. This also infers that the current component out of the accumulation layer in the conduction band is sensitively dependent on the tip's apex and its momentum-resolved density of states. Indeed, as shown in Fig. 1, we observed large differences in the magnitude of the current extracted from the accumulation layer for different tips, which otherwise show identical valence- and conduction-band-derived currents. This can be understood on the basis of tips accommodating better or worse electrons with large momentum parallel to the semiconductor surface.

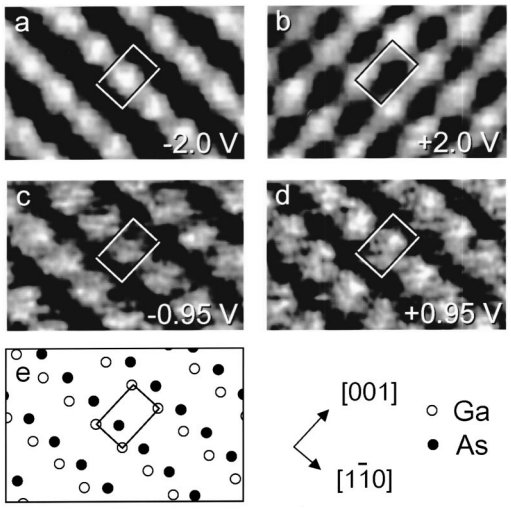

FIG. 8. Sets of STM images of the (110) surface of highly *p*-doped GaAs taken at −2.0 and +2.0 V (a), (b) and −0.95 and +0.95 V (c), (d) sample voltage. (e) Schematic drawing of the arrangement of the Ga (○) and As (●) atoms in the top layer of the GaAs (110) surface. The location of the box marks lattice positions identical in each set. It spans the size of a GaAs unit cell of 0.56 nm by 0.4 nm.

On basis of the importance of the momentum conservation in reducing the tunnel current extracted from the accumulation layer at negative voltages, we can conclude that the possibility of an atom-selective imaging of *n*-doped III-V compound semiconductor (110) surfaces depends crucially on the presence of an indirect surface band gap. If the minimum of the empty C_3 surface state would be at the $\bar{\Gamma}$ point of the surface Brillouin zone (direct surface band gap), then the current from the accumulation layer would dominate the STM images at all negative voltages and only the conduction-band surface states located at the cations would be imaged independent of the voltage. As a consequence, atom-selective imaging would be impossible. This situation could be the case for some II-VI semiconductor cleavage surfaces, e.g., *n*-doped ZnSe (110), where the few calculations of the surface band structure available suggest the possible presence of a direct surface band gap.[33,34]

VI. RESULTS AND DISCUSSION FOR *p*-TYPE GaAs

The tunneling conditions for *p*-doped GaAs are essentially analogous to the case of *n*-doped GaAs (exchange positive and negative voltages, as well as accumulation and inversion). In the following we will thus point out only the characteristics specific to *p*-type surfaces.

Figure 8 shows two sets of correlated high-resolution STM images of the highly *p*-doped GaAs (110) surface acquired at ±0.95 and ±2.0 V. The box marks a unit cell, whose position relative to the atomic lattice is the same in

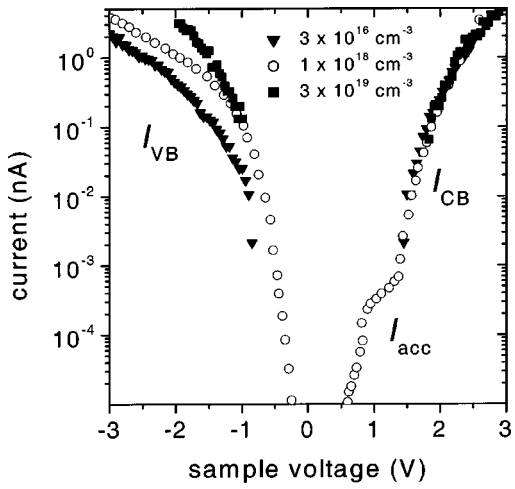

FIG. 9. Current-voltage data obtained on 3×10^{16} cm^{-3} (▼), 1×10^{18} cm^{-3} (○), and 3×10^{19} cm^{-3} (■) doped *p*-type GaAs. The data for the 1×10^{18} cm^{-3} doped sample is taken from Ref. 14. All curves are normalized to 0.2 nA at +2 V. The curves essentially overlap for positive voltages, whereas at negative voltages they are dependent on the doping concentration. At voltages $V>+1.4$ V, the current I_{CB} is dominated by electrons tunneling into the conduction band. For voltages $0\ \mathrm{V}<V<+1.4$ V, the current I_{acc} consists of electrons tunneling into the accumulation layer. For negative voltages the tunnel current stems from electrons tunneling out of the valence band (I_{VB}).

each set. The effects visible are analogous to those observed on *n*-type GaAs: At high voltages [Figs. 8(a) and 8(b)] the morphology and orientation of the apparent atomic rows rotates and the maxima are spatially shifting with opposite polarity. At negative voltages the atomic rows appear oriented along the $[1\bar{1}0]$ direction, whereas at +2.0 V they appear oriented along [001]. For small magnitudes of voltage the contrast and registry are essentially the same for either polarity [Figs. 8(c) and 8(d)].

At negative voltages, no inversion (gathering of electrons at the surface) can be expected for the same reasons as those discussed for *n*-doped material at positive voltages. For *p*-doped GaAs the free electrons cannot be transported from the bulk of the semiconductor to the surface. Therefore, only valence-band states are imaged at negative voltages. This is corroborated by the morphology observed in Fig. 8(a) that shows rows oriented along $[1\bar{1}0]$, which is characteristic for tunneling out of the anion-derived occupied A_5 dangling bond state in the valence band.[24,25] In addition, the tunneling current is strongly doping dependent (Fig. 9), because the tip's electric field is screened by the charged acceptors.

For a tunnel current at positive voltages, the filled states of the tip must face empty conduction- or empty valence-band states. Holes in the surface valence band (accumulation) can be expected starting at voltages at which the valence-band edge at the surface rises above the sample's Fermi level. This happens at $V\approx-(\Phi_m-\chi_{\mathrm{SC}})/e+E_g/e \approx+0.9$ V. With an accumulation layer formed, the band edges at the surface remain just slightly above their bulk values for even higher voltages and the tip's Fermi level rises above the surface conduction-band edge for $V\gtrsim+E_g/e=+1.42$ V. Therefore, the current observed for $+0.9\ \mathrm{V}\lesssim V\lesssim+1.42$ V in Figs. 8(d) and 9 (taken from Ref. 19) as well as Ref. 35 is due to electrons tunneling from the tip to valence-band states. The tunnel current at higher positive voltages is composed of two components: tunneling into empty conduction-band states and tunneling into emptied valence-band states. However, because the electrons tunneling into the conduction band have a larger transmission coefficient due to a smaller vacuum barrier height compared to those tunneling into the valence band, the first dominate in the STM images and in current-voltage curves (Fig. 9). Therefore, in Fig. 8(b) the morphology of the C_3 state is seen. The difference of the currents into the empty conduction and valence bands can be estimated to be three to four orders of magnitude. This is similar to the difference between I_{CB} and I_{inv} in Fig. 5 for the case of *n*-type GaAs.

At this stage it is should be noted that the small transmission coefficient for tunneling into and out of the valence-band states for *p*-type GaAs requires at voltages between −0.5 and +1.4 V small tip-sample separations in constant-current images. These small separations can cause tip-sample interactions[36] such that the gallium atoms are pulled out. Deformations of the surface bonds push the surface states energetically into the band gap,[37] and thus the images often display the anion and cation sublattices simultaneously.[38,39]

VII. DETERMINATION OF THE BAND GAP ENERGY

Without the tip-induced band bending (flatband assumption) a current-voltage curve would exhibit no current over a voltage range matching exactly the band gap energy divided by the elemental charge *e*. The previous discussion has clearly shown that tip-induced band bending modifies this simple picture. Thus the question remains as to how to extract the band gap energy from current-voltage spectroscopy data.

In the following we will show that the band gap energy E_g can be quite reliably obtained on *p*-type material from the strong (second) onset of the current at positive voltages. In Fig. 9 this is the onset at $V_p\approx+1.4$ V. As discussed above and schematically drawn in Fig. 10, at this voltage V_p the Fermi level of the tip $E_{F,\mathrm{tip}}$ rises above the conduction-band edge at the surface E_{CS}. Thus V_p can be written as $V_p=E_g/e-\Phi_{F,p}+\Phi_{\mathrm{acc},p}(V_p)$, with $\Phi_{F,p}$ the difference between the Fermi level of the semiconductor and the bulk valence-band edge, and $\Phi_{\mathrm{acc},p}(V)$ the amount of band bending in accumulation at voltage V (Fig. 10). Because of the high density of states at the valence-band edge, $d\Phi_{\mathrm{acc},p}/dV\approx0$ and $\Phi_{\mathrm{acc},p}(V_p)\approx\Phi_{F,p}\ll E_g$ at the onset of accumulation. Therefore, $V_p\approx E_g/e$. In addition, the onset at V_p is strong, because I_{acc} is, due to the small tunneling coefficient, small enough not to obstruct the onset (see Fig. 9). Notice that the onset V_p is essentially independent of the doping concentration, which is a requirement for an appropriate determination of the band gap energy.

In principle, one would expect to obtain the band gap energy in a symmetric manner on *n*-type GaAs, as $-V_n=E_g/e-\Phi_{F,n}+\Phi_{\mathrm{acc},n}(V_n)$ (Fig. 6). However, two factors complicate the determination of the band gap energy on

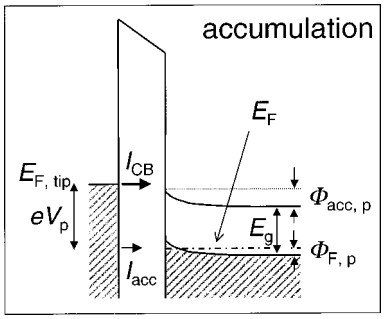

FIG. 10. Schematic band diagram of the metal-tip–vacuum–*p*-doped GaAs tunneling junction at the positive voltage (V_p), which corresponds to the onset of tunneling into the conduction band. The case with hole accumulation is shown. I_{acc} and I_{CB} denote the current from the filled tip states into the empty valence- and conduction-band states, respectively. $\Phi_{\mathrm{acc},p}$ is the difference in the band edge energies at the surface and the bulk. $\Phi_{F,p}$ is the difference between the Fermi level and valence-band edge in the bulk. E_g, $E_{F,\mathrm{tip}}$, and E_F, are the band gap energy, tip's Fermi level, and sample Fermi level, respectively.

n-type GaAs. First, $\Phi_{\mathrm{acc},n}(V_n) \gg \Phi_{F,n}(V_n)$, because $d\Phi_{\mathrm{acc},n}/dV$ is not negligible due to the smaller density of states at the conduction-band edge compared to the valence-band edge. Second, the stronger current component I_{acc} obstructs to some degree the onset of I_{VB} in the case of *n*-type GaAs (see Fig. 1).

VIII. CONCLUSION

In conclusion, we presented experimental and theoretical evidence that due to carrier dynamics no inversion occurs under tunneling conditions between a metal tip and *n*-type GaAs (110) surfaces at positive voltages. Thus all semiconductor states involved in the tunneling at positive voltages are conduction band related for *n*-type GaAs. We also presented experimental and theoretical evidence that accumulation occurs at negative voltages for *n*-type GaAs. A simple model that neglects momentum conservation would predict that tunneling out of conduction-band states would dominate over tunneling out of valence-band states and that consequently atom-selective imaging would not be possible on *n*-type GaAs. The discrepancy can be resolved if momentum conservation is included in the description of the tunneling current between the GaAs(110) surface and a metal tip. For the *p*-type GaAs(110) surface atom-selective imaging is possible, because at negative voltages all tunnel current originates from the valence band and at large positive voltages tunneling current to the conduction band dominates. This is due to the inability of the surface to form an inversion layer at negative voltages and because electrons tunneling into the conduction band see a vacuum barrier lower than those tunneling into the valence band at positive voltages. Based on the physical understanding of the states involved in the tunneling, we also developed a method to extract the band gap energy at unpinned surfaces.

ACKNOWLEDGMENTS

The authors would like to thank R. M. Feenstra and M. Salmeron for inspiring discussions and the Deutsche Forschungsgemeinschaft under Grant No. Eb 197/2-1 as well as the Director, Office of Energy Research, Office of Basic Energy Research, Materials Science Division, U.S. Department of Energy, under Contract No. DE-AC03-76SF00098 for financial support.

[1] H. Schmid, H. Stadler, and P. Varga, Phys. Rev. Lett. **70**, 1441 (1993).
[2] M. Pfister, M. B. Johnson, S. F. Alvarado, H. W. M. Salemink, U. Marti, D. Martin, F. Morier-Genoud, and F. K. Reinhart, Appl. Phys. Lett. **67**, 1459 (1995).
[3] K.-J. Chao, C.-K. Shih, D. W. Gotthold, and B. G. Streetman, Phys. Rev. Lett. **79**, 4822 (1997).
[4] J. F. Zheng, J. D. Walker, M. B. Salmeron, and E. R. Weber, Phys. Rev. Lett. **72**, 2414 (1994).
[5] S. L. Zuo, W. G. Bi, C. W. Tu, and E. T. Yu, Appl. Phys. Lett. **72**, 2135 (1998).
[6] J. Steinshnider, J. Harper, M. Weimer, C.-H. Lin, S. S. Pei, and D. H. Chow, Phys. Rev. Lett. **85**, 4562 (2000).
[7] B. Lita, R. S. Goldman, J. D. Phillips, and P. K. Bhattacharya, Appl. Phys. Lett. **75**, 2797 (1999).
[8] H. A. McKay, R. M. Feenstra, T. Schmidtling, U. W. Pohl, and J. F. Geisz, J. Vac. Sci. Technol. B **19**, 1644 (2001).
[9] A. J. Heinrich, M. Wenderoth, K. J. Engel, T. C. G. Reusch, K. Sauthoff, R. G. Ulbrich, E. R. Weber, and K. Uchida, Phys. Rev. B **59**, 10 296 (1999).
[10] R. M. Feenstra, J. A. Stroscio, J. Tersoff, and A. P. Fein, Phys. Rev. Lett. **58**, 1192 (1987).
[11] J. Tersoff and D. R. Hamann, Phys. Rev. B **31**, 805 (1985).
[12] L. J. Whitman, J. R. Stroscio, R. A. Dragoset, and R. J. Celotta, Phys. Rev. B **42**, 7288 (1990).
[13] Ph. Ebert, G. Cox, U. Poppe, and K. Urban, Surf. Sci. **271**, 587 (1992).
[14] N. D. Jäger, Ph. Ebert, K. Urban, R. Krause-Rehberg, and E. R. Weber, Phys. Rev. B **65**, 195318 (2002).
[15] J. F. Zheng, D. F. Ogletree, J. Walker, M. Salmeron, and E. R. Weber, J. Vac. Sci. Technol. B **12**, 2100 (1994). The electronic control is provided by RHK Technology, Inc.
[16] J. Frohn, J. F. Wolf, K. H. Besocke, and N. Teske, Rev. Sci. Instrum. **60**, 1200 (1989).
[17] S. Behler, M. K. Rose, D. F. Ogletree, and M. Salmeron, Rev. Sci. Instrum. **68**, 124 (1997).
[18] R. M. Feenstra, Phys. Rev. B **50**, 4561 (1994).
[19] R. M. Feenstra and J. A. Stroscio, J. Vac. Sci. Technol. B **5**, 923 (1987).
[20] R. Seiwatz and M. Green, J. Appl. Phys. **29**, 1034 (1958).
[21] J. Bono and R. H. Good, Jr., Surf. Sci. **175**, 415 (1986).
[22] A. Selloni, P. Carnevali, E. Tosatti, and C. D. Chen, Phys. Rev. B **31**, 2602 (1985).
[23] R. Maboudian, K. Pond, V. Bressler-Hill, M. Wassermeier, P. M.

Petroff, G. A. D. Briggs, and W. H. Weinberg, Surf. Sci. **275**, L662 (1992).
[24] N. D. Jäger, E. R. Weber, and M. Salmeron, J. Vac. Sci. Technol. B **19**, 511 (2001).
[25] Ph. Ebert, B. Engels, P. Richard, K. Schroeder, S. Blügel, C. Domke, M. Heinrich, and K. Urban, Phys. Rev. Lett. **77**, 2997 (1996).
[26] V. L. Dalal, A. B. Dreeben, and A. Triano, J. Appl. Phys. **42**, 2864 (1981).
[27] J. R. Chelikowski and M. L. Cohen, Solid State Commun. **29**, 267 (1979).
[28] A. Zunger, Phys. Rev. B **22**, 959 (1980).
[29] C. Mailhiot, C. B. Duke, and D. J. Chadi, Phys. Rev. B **31**, 2213 (1985).
[30] X. Zhu, S. B. Zhang, S. G. Louie, and M. L. Cohen, Phys. Rev. Lett. **63**, 2112 (1989).
[31] J. L. A. Alves, J. Hebenstreit, and M. Scheffler, Phys. Rev. B **44**, 6188 (1991).
[32] B. Engels, P. Richard, K. Schroeder, S. Blügel, Ph. Ebert, and K. Urban, Phys. Rev. B **58**, 7799 (1998).
[33] J. L. A. Alves, K. Watari, and A. C. Ferraz, Braz. J. Phys. **24**, 99 (1994).
[34] C. Calandra, F. Manghi, and C. M. Bertoni, J. Phys. C **10**, 1911 (1977).
[35] S. Aloni and G. Haase, J. Vac. Sci. Technol. B **17**, 2651 (1999).
[36] S. H. Ke, T. Uda, R. Pérez, I. Štich, and K. Terakura, Phys. Rev. B **60**, 11 631 (1999).
[37] D. J. Chadi, Phys. Rev. B **18**, 1800 (1978).
[38] N. D. Jäger, X. Liu, J. F. Zheng, N. Newman, D. F. Ogletree, E. R. Weber, and M. Salmeron, in *Proceedings of the 23rd International Conference on the Physics of Semiconductors*, edited by M. Scheffler and R. Zimmermann (World Scientific, Berlin, 1996), Vol. 2, p. 847.
[39] A. J. Heinrich, M. Wenderoth, M. A. Rosentreter, M. A. Schneider, and R. G. Ulbrich, Appl. Phys. Lett. **70**, 449 (1997).